PHYSICAL REVIEW D VOLUME 43, NUMBER 7 1 APRIL 1991

Fragmentation of color strings

H. J. Schulze and J. Aichelin
Institut für Theoretische Physik der Universität Heidelberg, and Max-Planck-Institut für Kernphysik, D-6900 Heidelberg, Germany
(Received 26 June 1990)

The fragmentation of a color string, formed in e^+e^-, μp, and pp collisions, is assumed to be a sequence of phase-space-dominated binary decays: string→string+hadron. This model requires only one parameter, the average transverse momentum, and describes a wealth of recently measured e^+e^-, μp, and pp data, such as multiplicity and momentum distributions, the number of created resonances, and the scale breaking of the momentum distribution at low Feynman x. To avoid ambiguities for the string formation in pp collisions we develop a method to calculate the transverse-momentum distribution of partons from the longitudinal-momentum distribution which is based on symmetry arguments only.

I. INTRODUCTION

When highly accelerated particles such as protons, muons, or electrons collide one observes that many hadrons are produced. What do these particles reveal about their production mechanism? Can we learn something about the underlying QCD, for example, by realizing that the process is governed by counting rules? Are there similarities between the production of hadrons in e^+e^- collisions, where all the energy is stored in the virtual photon, deep-inelastic μp collisions, where the momentum transfer is large, and pp collisions, where in the majority of the events the momentum transfer is rather small and therefore the strong coupling constant α_s is large?

These questions have first been investigated by comparing experiments with the longitudinal-phase-space model:[1] In the oldest uncorrelated-jet models it is assumed that the particles which emerge from the particle production process are uniformly distributed in longitudinal phase space, i.e., the relativistically invariant momentum space weighted with some empirical function which restricts transverse momenta. Thus in a phenomenological way these models take the longitudinal structure of the experimentally observed events into account. Because of the multitude of different channels the final distribution of hadrons is hard to calculate in this approach and therefore usually only approximate solutions were obtained. Restricted to production of only one kind of particles (pions) these models yield asymptotic scaling behavior of the inclusive momentum distributions and a logarithmic rise of mean multiplicity with event energy, but fail to reproduce other results such as the absolute value of the number of produced hadrons. Recently, the predictions of the model were compared in detail with data employing a grand canonical approximation and allowing the production of pions, kaons, protons, and Λ's.[2]

More refined models assume that the production of hadrons is a two-step process:[3] A first initial step in which color strings are formed is followed by the decay of the strings into hadrons. The string formation in proton induced reactions is determined by the measured structure functions; the fragmentation, by fragmentation functions. The latest and most frequently used models of this kind are the LUND,[3] and the dual-parton model.[4] Whereas in e^+e^- and μp collisions the formation of the color string is the same in both models, the formation of strings in pp collisions requires assumptions about the soft interactions between the partons of the different protons. In the LUND model, momentum but no color is exchanged; the dual parton model assumes just the opposite. However, the practical differences of the formation process are of minor importance because it turns out that independent of the assumed process for the string formation the distribution of the invariant masses of the strings is almost identical.

Of more importance is the physics of the fragmentation process. All these models assume that the string decay reveals some information about the underlying QCD, i.e., is not completely phase-space dominated. Originally, Field and Feynman[3] introduced the idea of quark-antiquark pair production in the color string and recombination to the observed mesons, obtaining a sequential decay of the string. In the models used nowadays, higher-mass mesons and baryons are produced also. Parameters determine whether a meson or baryon is produced, the flavor of the produced $q\bar{q}$ pair(s), and the spin of the produced hadron. These parameters are adjusted to reproduce data. In the LUND model, this sequential structure of the decay is related to the space-time evolution of the fragmentation via the relation $p^+=\kappa x^+$, where κ is the string constant and x^+ and p^+ are the light-cone position and momentum. Fragmentation functions $f(p^+/p^+_{\max})$ are used to generate the light-cone momentum fraction of the created hadrons. Thus for a given transverse mass m_T of the hadron, $x^-=m_T^2/\kappa^2 x^+$ and therefore the space-time point of the creation is determined. The fragmentation functions are based on counting rules, i.e., the momentum distribution of the produced hadrons is determined by the number of spectator quarks. In addition there is a low-momentum suppression for diquark and heavy-quark fragmentation. The flavor of the produced quark-antiquark pair is governed by a strangeness-suppression factor and a

vector-meson-dominance factor is included also.

With about 6 to 8 parameters which are independent of the entrance channel, both models describe beautifully the momentum distributions of different species and the multiplicity distributions of e^+e^-, μp, and pp data. These models are easily extended to hadron-nucleus and nucleus-nucleus collisions,[5] however at the price of introducing further parameters. Additional parameters are also required if one would like to study the production of heavier resonances.

Our aim is different. Instead of trying to fit the data by introducing a lot of parameters we want to study to which degree a simple and well-defined, but not necessarily quite realistic, model describes the data. Our model is based on the assumption that the distribution of particles is completely determined by the longitudinal phase space. In view of Fermi's golden rule this assumption implies that the transition matrix between initial and final state, which contains all the QCD implications, is constant. This is of course a strong assumption, which however was quite successful in other field of physics where one faced the same problem, namely that the transition matrix is too complicated to be calculated. It can be viewed as a minimal-information ansatz.

Usually it is assumed that phase-space dominance specifies the model completely. This, however, is not true because one has to specify the initial and final state. There are two alternatives. Either the n-body final state is produced instantaneously, which is assumed in the so-called longitudinal-phase-space models, or the n-body final state is produced by the sequential decay of the source, where in between the decay steps the system equilibrizes, i.e., loses its memory on previous steps. We will adopt the second alternative. Thus our model differs from the usual longitudinal-phase-space model and it is bound to give different results, as we will see in the second section. To be more specific: We start from the one assumption that a color string hadronizes in a sequence of binary decays string$\rightarrow$string+hadron. Each decay step is determined by the longitudinal phase space and an assumed Gaussian distribution of the transverse momentum. This distribution requires one input parameter $\langle p_T^2 \rangle$.

This approach has immediately two implications. (a) Because of the constant transition matrix element gluons do not appear explicitly in this approach. As particles which cause the interaction they are only responsible for the equilibration. (b) The observed short-range charge correlation is mainly due to heavy-meson decay (only less than 50% of the observed final particles do not come from the decay of heavy resonances). Only a smaller fraction comes from correlations between subsequent decay steps (the latest produced meson must have correct quantum numbers, which implies constraints on the previous decay steps).

If our model reproduces the measured quantities such as multiplicity distributions, momentum distributions, and the dependence of all these quantities on the string energy, then this means that the data are compatible with the assumption that the transition matrix elements are constant, thus questioning conclusions of other models that the hadronization of strings reveals something about QCD. Only if it disagrees is there room for undoubtable QCD effects. Originally our intention was to search for these discrepancies.

To our big surprise the agreement of this simple model with data goes much beyond what we expected. The level of agreement with data is as good as that of the so-called event generators such as VENUS or HIJET.[3,4] Only the LUND model, following the strategy to force agreement by fit parameters, gives better results. Even more, experimental observation such as scale breaking of the momentum distribution of the produced mesons at low energy or the ratio of strange to nonstrange particles can be shown to be enforced by phase space only.

Unfortunately there are some obstacles to carry through this approach in practice. In principle we have to know the masses, the degeneracy, and the decay channels of all possible hadrons. These are not known for hadrons with the mass of the lightest baryon. This requires one additional parameter for actual calculations, the baryon-to-meson ratio. This parameter is the same for e^+e^-, μp, and pp reactions.

For comparison with experiments we employ a Monte Carlo procedure. However, a slightly simplified version of the string decay model can be calculated analytically.[6] The analytical solution makes the essential features quite transparent; in particular it shows the origin of the scaling violation at low hadron energies and the influence of the resonances on the final momentum spectra.

This model has been successfully applied to the e^+e^- data in the range from 14 to 34.5 GeV.[6] It reproduced experimental multiplicity distributions, the momentum distributions of different hadrons and the production of resonances such as ρ, K^*, and η. Thus it allowed us the conclusion that the combination of a vector-dominance parameter, the strangeness-suppression factor, and the fragmentation function produces the same distributions as a phase-space-dominated sequential decay. The only discrepancies between experiment and calculation showed up at the expected places, where the experimentally observed three-jet events are important which are neglected in our approach.

In this article we continue our investigation. We compare our results with data of the European Muon Collaboration (EMC) and with pp data. The article is organized as follows.

In Sec. II we investigate the differences between an instantaneous and a sequential decay of a color string, both governed by longitudinal phase space. For this purpose we introduce a toy model which allows us to investigate analytically the differences in the number of produced particles and the momentum distributions which can be observed in the much more elaborate exact calculations.

In Sec. III we introduce our model. We display in detail the formalism and give analytical approximations. We briefly repeat the main results for the e^+e^- annihilation of Ref. 6.

In Sec. IV we derive a method of calculating the transverse-momentum distribution of partons from a given longitudinal-momentum distribution. This relation between transverse and longitudinal momentum enables

us to avoid ambiguities in the formation of strings created in μp and pp collisions.

In Secs. V and VI we apply our model to deep-inelastic muon-proton scattering and soft proton-proton collisions and compare the results with experimental data. We treat the string formation processes in lowest order, using the impulse approximation for deep-inelastic μp scattering and the dual-parton model for inelastic pp collisions.

In Sec. VII we draw our conclusions.

II. SEQUENTIAL VERSUS INSTANTANEOUS DECAY

The longitudinal-phase-space model assumes that the hadrons created in a highly energetic reaction are produced simultaneously. All many-particle final states which are compatible with the conservation laws are allowed. The single-particle distributions of hadrons are obtained by summing over all possible many-hadron final states with a weight that limits the transverse momenta of the particles. In practice there are infinitely many final states and one has to make approximations for calculating the spectra. One approximation which allows even analytical results is the discretization of the longitudinal momentum in bins of fixed Δy.[2]

There is, however, a second process which can also be completely phase-space dominated: the sequential decay of a highly excited object. Between the different decay steps the system equilibrates completely, i.e., populates all states which are compatible with the conserved quantities. Thus it has lost its memory of having a predecessor. In nuclear physics this sequential-decay mechanism (compound nucleus model) was introduced by Weisskopf[7] already in the 1930's and has been proven to describe moderately excited nuclei which decay by emission of light particles and photons. We assume that also a color string decays sequentially and each decay step is dominated by the longitudinal phase space.

At first sight it is not obvious whether the spectra of the produced particles depend on being emitted in an instantaneous or in a sequential decay. To point out the difference we employ a toy model which bears, however, all the essential physics. In this toy model we neglect the momentum completely and assume that the energy is quantized in units of 1. Furthermore we allow only one kind of particle. The particles are assumed to be indistinguishable.

If we have initially $N=4$ units of energy which can be carried away by a unlimited number of particles, the following decay channels are possible in an instantaneous decay: (4),(3,1),(2,2),(2,1,1),(1,1,1,1). Each channel has the same weight. The relative ratio of particles with 1, 2, 3, and 4 units of energy is 7:3:1:1. The probability of finding a particle which carries all the energy is one over the number of different decay channels [i.e., $1/P(N), P(N)$ being the number of ordered partitions of the number N].

Let us now investigate the sequential decay. We assume that the emission probability is independent of the number of energy units the particle carries away. The possible decay sequences are shown in Fig. 1. Collecting now all the decay channels we find that the relative probability of particles with 1, 2, 3, and 4 units of energy is 12:6:4:3. The probability of finding a particle which carries all 4 energy units is $1/N$.

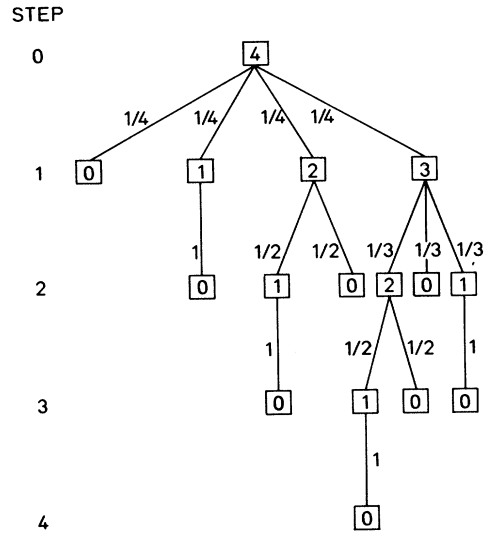

FIG. 1. Sequential decay paths in the toy model. We start with four units of energy. The number in the box marks the number of energy units left after each decay step. The numbers close to the lines mark the probabilities.

$P(N)$ increases much faster than linear. Hence a sequential decay on the average produces more particles with less average energy than an instantaneous decay. In Ref. 2 it has been found that the number of particles obtained in an instantaneous decay is too low and the longitudinal-momentum distribution too flat. Both features can be expected to be improved in a sequential-decay model.

III. THE MODEL

Our phase-space-dominated sequential-decay model has two steps: an initial formation step in which a string of a given energy is formed and the decay step in which the decaying string produces a sequence of hadrons. The formation step depends on the reaction investigated. In e^+e^- annihilation the quark-antiquark strings are produced with the relative probability $u\bar{u}:d\bar{d}:s\bar{s}:c\bar{c}:b\bar{b}$ $=1:4:1:4:1$. The decay of strings with heavy leading quarks starts with the decay into a heavy B or D meson. In pp and μp collisions quark-diquark strings are formed. The way they are produced will be explained in the next section. The diquark string is assumed to emit a baryon first. Hence after the first emission step the strings do not carry information on the production process anymore. The subsequent steps are identical for all strings.

We assume that the string with the initial mass $M_0=\sqrt{s}$ decays in a sequence of binary decays. In each decay step an on-shell hadron is produced and a string with less energy and a recoil momentum is left:

$$\underbrace{\text{string}(M_{i-1})}_{i} \rightarrow \underbrace{\text{string}(M_i)+\text{hadron}(m_i)}_{f} . \tag{1}$$

The probability for the decay of the string M with momentum P into a string with momentum Q and a hadron m with momentum p is given by Fermi's golden rule:

$$d^3\Gamma_{Mm}(P \to Q+p) = |M_{Mm}|^2 d^4Q\, d^4p \ . \tag{2}$$

Defining

$$|M_{Mm}|^2 \equiv 2f_{Mm}(y,\mathbf{p}_T)\delta^4(P-Q-p)\delta(p^2-m^2) \ , \tag{3}$$

we obtain

$$d^3\Gamma_{Mm}(P \to Q+p) = f_{Mm}(y,\mathbf{p}_T)dy\, d^2\mathbf{p}_T \ . \tag{4}$$

Here the fragmentation function $f_{Mm}(y,\mathbf{p}_T)$ gives the probability for the emission of a hadron m with rapidity y and transverse momentum $\mathbf{p}_T$ from the string M. If the string decay were completely dominated by phase space, f_{Mm} would be constant in the allowed kinematical region and zero otherwise. Experiments show that the observed events have a longitudinal structure. We take this observation into account by limiting the transverse momentum of the produced hadron. We assume a Gaussian form of the transverse-momentum distribution which requires the average squared transverse momentum as an input parameter. This parameter is kept constant for all produced particles and for all different reactions. Thus our fragmentation function has the form

$$f_{Mm}(y,\mathbf{p}_T) = C_M S_m \exp(-p_T^2/\lambda)\Theta(M/2 - m_T\cosh y) \ . \tag{5}$$

Here the C_M is a normalization constant, $S_m=(2J_m+1)(2I_m+1)$ is a statistical factor (J_m and I_m are spin and isospin of the hadron m), the Θ function expresses energy conservation, and the Gaussian restricts the transverse momenta. The parameter λ is fixed to 0.8 $(\text{GeV}/c)^2$. In our phase-space approach the fragmentation function is independent of the rapidity y. This is also a result of the (1+1)-dimensional Schwinger model,[8] giving our assumption a better founded theoretical basis.

Neglecting the kinematical boundary $p_{T_{\max}}(y)$, the probability for emission of a hadron m from the string M is then given by the available longitudinal phase space:

$$\Gamma_{Mm} = \int dy\, d^2\mathbf{p}_T C_M S_m \exp(-p_T^2/\lambda)\Theta(M/2 - m_T\cosh y)$$
$$\approx C'_M S_m y_{\max}(M,m) \ , \tag{6}$$

where

$$y_{\max}(M,m) = \operatorname{arccosh}\left[\frac{M}{2m}\right] \tag{7}$$

and

$$C'_M = \frac{1}{\sum_m S_m y_{\max}(M,m)} \ . \tag{8}$$

Hence mesons and baryons fragment in the same way in this approach. The larger the mass of a hadron, the smaller is the probability that it is produced. Therefore baryons are less copiously created than mesons and the lower production rates of strange, charmed, and beauty particles are only due to their higher mass. The conservation of baryon number, flavor, and charge is ensured by producing baryon and antibaryon and meson and its flavor partner in pairs.

We still have to specify the hadrons m which are produced in our model. As an extreme, all resonances and all baryons up to $m < M/2$ should be allowed. For practical reasons this is not possible: the resonance density $\rho(m)$ rises exponentially and decay channels and fractions of the high-lying states are not known. Therefore in our calculation we take into account the primary production of pseudoscalar and vector mesons and the baryon octet, i.e.,

$$m = \begin{cases} \pi,\eta,\eta',K,D,D_s,B,B_s,\rho,\phi,\omega,K^*,D^*,D_s^*,B^*,B_s^* \\ \hfill (\text{meson}) \ , \\ N,\Lambda,\Sigma,\Xi \quad (\text{baryon}) \ . \end{cases} \tag{9}$$

The final-state particles are obtained by letting the directly produced resonances decay according to the Particle Data Group tables. We checked in which way the limitation of resonances influences the results. For this purpose we included the tensor mesons in our calculation. We found that the resulting distributions of observed particles [charged pions, kaons, and (anti)protons] are rather insensitive to their inclusion. The main influence of the resonance decay is a slight depopulation of the large-Feynman-x region, because the momentum of the resonance is divided among its decay particles and spread in transverse direction. There is, however, an observable which is influenced by the limitation of the resonances: The baryon-to-meson ratio depends of course on the number of resonances taken into account. With our choice of resonances we obtain the correct meson-to-baryon ratio. Thus this ratio is not predicted by our model but is an input.

A simplified version[6] of the model allows for analytical calculation. Here we assume that only one kind of particle (pion) is produced with a fixed transverse mass $m_T = \langle m_T \rangle$. The energy is conserved in the mean and the recoil is neglected. The average energy the produced hadron carries away in the ith fragmentation step is given by

$$\langle \Delta M_i \rangle = \int_{m_T}^{M_i/2} P(E)E\, dE \approx \frac{M_i(\frac{1}{2} - m_T^2/M_i^2)}{\ln(M_i/m_T)} \ , \tag{10}$$

where M_i is the mass of the string prior to the ith fragmentation step. This relation can be cast into a differential equation with the solution

$$\langle N \rangle = \int_{m_T}^{M_0/2} \frac{\ln(M/m_T)}{M(\frac{1}{2} - m_T^2/M^2)} dM \ . \tag{11}$$

In agreement with the experimental observation the mean multiplicity increases in between:

$$\text{const}\times\ln\left[\frac{M_0}{2m_T}\right]^2 < \langle N \rangle(M_0) < \text{const}\times\ln^2\left[\frac{M_0}{2m_T}\right]^2 . \tag{12}$$

In this simplified model we obtain also the Feynman scal-

ing of the longitudinal-momentum distribution for large Feynman $x = 2p_L/M_0$ and the breakdown of the scaling at low x:

$$\frac{dN_{\rm ch}}{dx}(x) = \frac{2}{3}\left[\frac{M_0}{2E(x)}\right]\ln\left[\frac{M_0}{2E(x)}\right] = -\frac{2}{3}\frac{\ln\sqrt{x^2+(2m_T/\sqrt{s})^2}}{\sqrt{x^2+(2m_T/\sqrt{s})^2}} . \quad (13)$$

Not only in its functional dependence but also in the absolute values, the approximate solution comes very close to the Monte Carlo result and to the data. This means that resonance decay as well as the distribution of the transverse momenta are only of minor importance and only necessary for a careful comparison with data. The bulk properties like the form of inclusive momentum distributions and multiplicity distribution are almost completely fixed by the fundamental ansatz of a sequential phase-space-dominated decay of the string.

The results of our model have been compared with the published data of the TASSO group in the energy range between 14 and 34.5 GeV. Here we repeat the main results only.[6]

(1) The pion-to-kaon ratio was exactly obtained and the experimental mean multiplicities of higher resonances η, ρ_0, K^* were fairly well described, which means that the strangeness suppression is a consequence alone of the higher mass of strange hadrons.

(2) Although the momentum distribution of protons was well reproduced, we obtained a proton-to-Λ ratio of 1:1 in contrast with the experimental value of 3:1.

(3) All inclusive momentum distributions and the multiplicity distribution were in perfect agreement with experiment at $\sqrt{s} = 14$ GeV. In particular, the "seagull" shape of the $\langle p_T \rangle(x)$ plot was shown to be a consequence of the sphericity analysis, which considerably lowers the transverse momenta of the observed charged particles.

(4) At 34.5 GeV we saw first discrepancies between theory and experiment; namely, the transverse momenta (with respect to the sphericity axis) of the produced particles were too small, which led to a p_T distribution that fell too steeply, and a too low $\langle p_T \rangle(x)$. This is supposedly a consequence of neglecting three-jet events, the inclusion of which should modify the mentioned observables in the right way. Nevertheless, the longitudinal-momentum distributions were hardly influenced by this.

IV. CORRELATIONS BETWEEN LONGITUDINAL- AND TRANSVERSE-PARTON-MOMENTUM DISTRIBUTIONS

The simulation of the μp and the pp scattering events requires the knowledge of the longitudinal- and transverse-momentum distributions of the partons inside the proton. In μp collisions a finite transverse momentum of the parton causes the jet axis not to be identical with the photon direction. In pp collisions the influence is even bigger. Most of the partons have very small longitudinal momenta. Hence the mass of a formed string depends decisively on the transverse momentum of the parton. Therefore a reliable way of obtaining information on the transverse-momentum distribution as a function of x_L is needed. We will show in this section that the assumption of an isotropic momentum distribution of the partons in the rest system of the proton produces correlations between the longitudinal- and the transverse-momentum distributions, and in particular that it is sufficient to know the longitudinal-momentum distribution in order to reconstruct the required distribution $f(p_T, x_L)$.

We assume that on a "resolution scale" $1/Q$ the momentum distribution of a certain kind of parton is spherically symmetric in the rest system of the proton:

$$\frac{d^3n}{d^3\mathbf{k}}(\mathbf{k}) = \frac{dn}{4\pi k^2 dk}(k), \quad k \equiv |\mathbf{k}| . \quad (14)$$

Note that the scale Q is treated as an external parameter of the distribution function and is always suppressed in the following. We do not consider a proportionality between Q and the maximum resolved transverse momentum of the partons.[9] Rather, we investigate the consequences of the assumption of an isotropic momentum distribution in the rest system of the proton.

The partons are treated as massless. Because of four-momentum conservation the parton momentum is then limited to

$$k_{\rm max} = \frac{M_{\rm proton}}{2} . \quad (15)$$

The symmetry of the distribution function is now translated to light-cone coordinates:

$$k^{\pm} = k_0 \pm k_L \Longrightarrow k^- = \frac{k_T^2}{k^+} . \quad (16)$$

With this transformation, spheres of constant parton energy k_0 in $(k_L, \mathbf{k}_T)$ coordinates are mapped to shifted spheres in $(k^+, \mathbf{k}_T)$ coordinates as indicated in Fig. 2. Therefore the kinematical boundary for parton transverse momenta dependent on their light-cone momentum is

$$k_{T\max}(k^+) = \sqrt{k^+(M-k^+)} , \quad (17)$$

and the distribution function transforms as

$$\frac{d^3n}{dk^+ d^2\mathbf{k}_T} = \frac{d^3n}{dk_L d^2\mathbf{k}_T}\frac{\partial k_L}{\partial k^+} \Longleftrightarrow \frac{d^2n}{dk^+ dk_T} = \frac{k_T}{2kk^+}\frac{dn}{dk} . \quad (18)$$

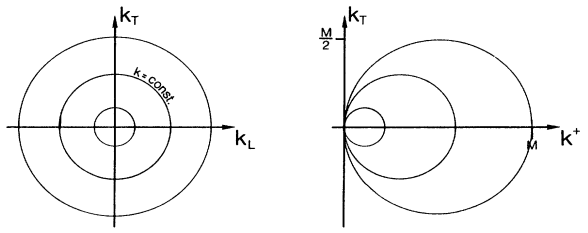

FIG. 2. Transformation from momenta to light-cone momenta. The circles mark constant parton energy.

For convenience, we introduce dimensionless, boost-invariant variables

$$x \equiv x^+ = \frac{k^+}{M}, \quad y \equiv \frac{k_T}{M}, \quad E \equiv \frac{k}{M}, \tag{19}$$

and obtain

$$\frac{d^2n}{dx\,dy}(x,y) = \frac{y}{2xE}\frac{dn}{dE}(E(x,y)), \quad E(x,y) = \frac{x^2+y^2}{2x}. \tag{20}$$

This result relates the double-differential momentum distribution and the energy distribution of the partons. The longitudinal parton density is then

$$f(x) \equiv \frac{dn}{dx}(x) = \int_0^{y_{\max}(x)=\sqrt{x(1-x)}} dy \frac{d^2n}{dx\,dy}(x,y)$$
$$= \int_{E_{\min}(x)=x/2}^{E_{\max}(x)=1/2} dE \frac{1}{2E}\frac{dn}{dE}(E)$$
$$\Longleftrightarrow 2f'(x) = -\frac{1}{2E}\frac{dn}{dE}(x/2) \tag{21}$$
$$\Longleftrightarrow \frac{dn}{dE}(E) = -4Ef'(2E)\,. \tag{22}$$

Now the double-differential momentum distribution can be expressed as a functional of the (known) longitudinal-momentum distribution of the partons:

$$\frac{d^2n}{dx\,dy}(x,y) = -\frac{2y}{x}f'(2E) = -\frac{2y}{x}f'\left[\frac{x^2+y^2}{x}\right]$$
$$= -\frac{d}{dy}f\left[\frac{x^2+y^2}{x}\right]. \tag{23}$$

This result in the form of a derivative is particularly convenient for the Monte Carlo generation of the transverse momentum y for a given light-cone momentum x; namely, it reduces to the task of finding the zero of the function

$$f\left[\frac{x^2+y^2}{x}\right] - z\,,$$

where z is distributed randomly in $[0, f(x)]$. Employing partial integration and the experimentally known fact that

$$x^2 f(x)|_{x=0} = 0 \tag{24}$$

for all kinds of partons, we can calculate moments of the distributions:

$$\langle E \rangle = \int_0^{1/2} dE \frac{dn}{dE}(E)E = \langle x \rangle\,, \tag{25}$$

$$\langle E^2 \rangle = \int_0^{1/2} dE \frac{dn}{dE}(E)E^2 = \tfrac{3}{4}\langle x^2 \rangle\,, \tag{26}$$

$$f(x)\langle y \rangle(x) = \int_0^{y_{\max}(x)=\sqrt{x(1-x)}} dy \frac{d^2n}{dx\,dy}(x,y)y$$
$$= \int_0^{\sqrt{x(1-x)}} dy\, f\left[\frac{x^2+y^2}{x}\right], \tag{27}$$

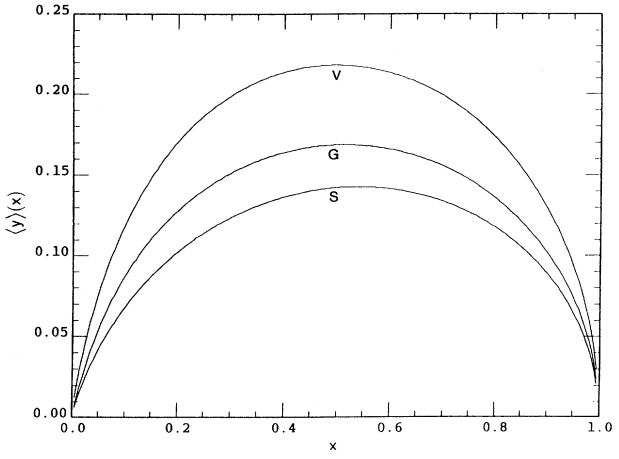

FIG. 3. The dependence of mean parton transverse momentum $y = |\mathbf{k}_T|/M$ on light-cone momentum $x = k^+/P^+$ for valence quarks, sea quarks, and gluons.

$$f(x)\langle y^2 \rangle(x) = \int_0^{y_{\max}(x)=\sqrt{x(1-x)}} dy \frac{d^2n}{dx\,dy}(x,y)y^2$$
$$= x\int_x^1 dx' f(x')\,, \tag{28}$$

$$\langle y \rangle = \int_0^1 dx\, f(x)\langle y \rangle(x) = \frac{\pi}{4}\langle x \rangle\,, \tag{29}$$

$$\langle y^2 \rangle = \int_0^1 dx\, f(x)\langle y^2 \rangle(x) = \tfrac{1}{2}\langle x^2 \rangle\,. \tag{30}$$

For illustration we show in Fig. 3 the dependence of the mean transverse momentum $\langle y \rangle$ on light-cone momentum x for the different parton species, using the parametrizations of Duke and Owens[10] at $Q^2 = 4$ (GeV/c)^2:

$$f_V(x) = 1.88x^{-0.58}(1-x)^{3.46}(1+4.4x)\,,$$
$$f_S(x) = 1.27x^{-1}(1-x)^{8.05}\,, \tag{31}$$
$$f_G(x) = 1.56x^{-1}(1-x)^{6.0}(1+9.0x)\,.$$

We remark that similar results for $\langle y \rangle(x)$ [Eq. (27)] were once obtained by Glück and Reya.[11]

V. APPLICATION TO MUON-PROTON SCATTERING

The scattering event is treated in the impulse approximation (Fig. 4): the incoming muon of energy E ex-

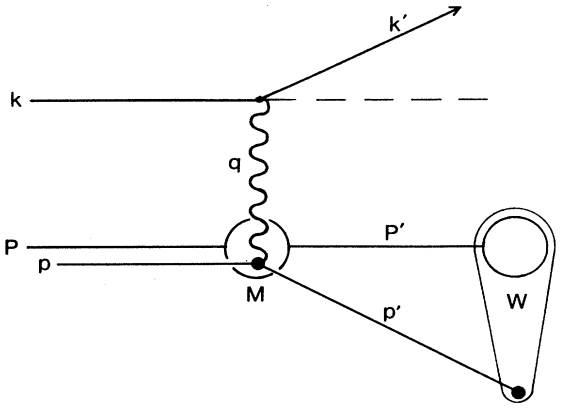

FIG. 4. Muon-proton scattering in the impulse approximation.

changes a virtual photon of mass $q^2=-Q^2$ with a parton p of the target nucleon P. The parton is kicked out of the nucleon and a string of mass $W^2=(P+q)^2$ is formed. It connects the parton and the target remnant, called the diquark.

The differential cross section for this process is

$$\frac{d^2\sigma}{dW^2dQ^2}=4\pi\alpha^2F_2\frac{x_B}{Q^6}\left[1-y_B-\frac{Q^2}{4E^2}+\frac{y_B^2+Q^2/E^2}{2(1+R)}\right], \tag{32}$$

with

$$x_B(W^2,Q^2)=\frac{-q\cdot q}{2q\cdot P}=\frac{Q^2}{W^2-M^2+Q^2}, \tag{33}$$

$$y_B(W^2,Q^2)=\frac{q\cdot P}{k\cdot P}=\frac{W^2-M^2+Q^2}{2ME}, \tag{34}$$

$$\nu(W^2,Q^2)=\frac{q\cdot P}{M}=\frac{W^2-M^2+Q^2}{2M}, \tag{35}$$

and $F_2(Q^2,W^2)$ and $R(Q^2,W^2)$ are structure functions. These have been measured and parametrized by[12] the EMC at $E=280$ GeV. We use their parametrization to generate events in the Q^2,W^2 plane, restricted by the same kinematical cuts as were done experimentally.

The relation between the kinematical variables Q^2,W^2 and the momentum p of the struck parton is given in the naive parton model through the mass-shell condition $p^2=(p+q)^2=0$ as

$$x_B(Q^2,W^2)=\frac{2q\cdot p}{2q\cdot P}=\frac{1}{2}\left[x^+ +\frac{p_T^2}{x^+M^2}\right]+\frac{1}{2}\left[x^+-\frac{p_T^2}{x^+M^2}\right]\left[1+\frac{Q^2}{\nu^2}\right]^{1/2}, \tag{36}$$

which for $\nu\gg Q$ (well satisfied for the treated kinematical region) reduces to the well-known $x_B=x^+$. Here x^+ and $\mathbf{p}_T$ are light-cone momentum fraction and transverse momentum of the parton relative to the axis of the incoming photon. Because of the transverse momentum the string axis is rotated against the (experimentally known) photon axis by $\varphi\approx\arcsin(2p_T/W)$ (Fig. 5). We generate the transverse momentum of the struck parton in the way described in the preceding section. Assuming a spherically symmetric momentum distribution in the rest system of the proton we can get, from the longitudinal parton density,

$$\frac{dn}{dx^+}(x^+,Q^2)\equiv f(x^+,Q^2)=\sum_{\text{flavors}}e_f^2[q_f(x^+,Q^2)+\bar{q}_f(x^+,Q^2)]=\frac{F_2(x^+,Q^2)}{x^+} \tag{37}$$

the parton momentum distribution [Eq. (23)]

$$\frac{d^2n}{dx\,dy}(x,y,Q^2)=-2\frac{y}{x}f'\left[\frac{x^2+y^2}{x},Q^2\right],$$

$$\text{where } x=x^+,y=\frac{p_T}{M}. \tag{38}$$

Therefore the knowledge of $F_2(x,Q^2)$ is sufficient to generate the parton transverse momentum for an event characterized by $x_B(Q^2,W^2)$.

In contradistinction to an e^+e^- collision in which a quark-antiquark string is formed in deep-inelastic lepton scattering we produce a quark-diquark string. Baryon-number conservation requires that at least one baryon has to be produced in the fragmentation. Two simple fragmentation scenarios are possible. Either the color string connects the struck parton with the diquark or the struck particle drags along an antiquark leaving behind an excited color neutral object with the baryon number 1. Both together are color neutral and an only mildly excited baryon is left. The latter process would explain why the kinetic energy of the proton in the laboratory system is of the order of some tens of MeV as compared to the total string energy of more than 10 GeV. A detailed investigation which process is most probable would require proton data with exact Q^2 and W^2 values which are not available.

The second process requires the knowledge of a two-parton distribution function which is not known. The first process alone, which requires only the one-parton

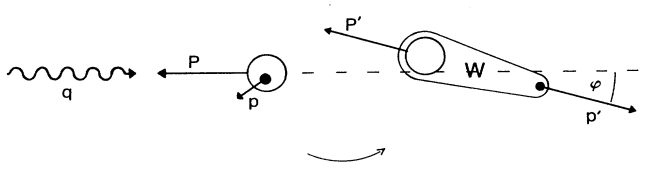

FIG. 5. Rotation of the string axis against the axis of the virtual photon.

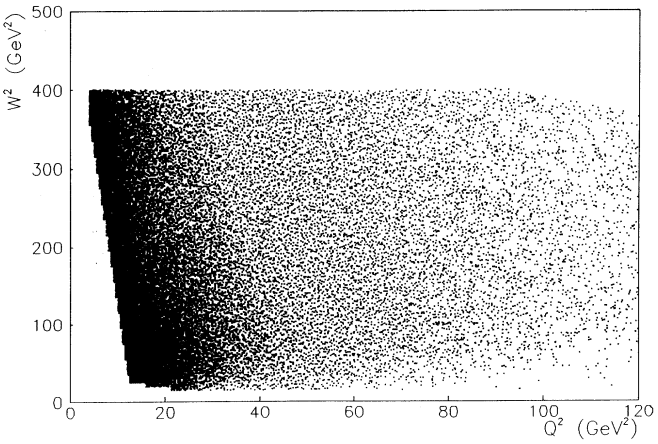

FIG. 6. Scatter plot of the generated events for the 280-GeV muon-proton scattering.

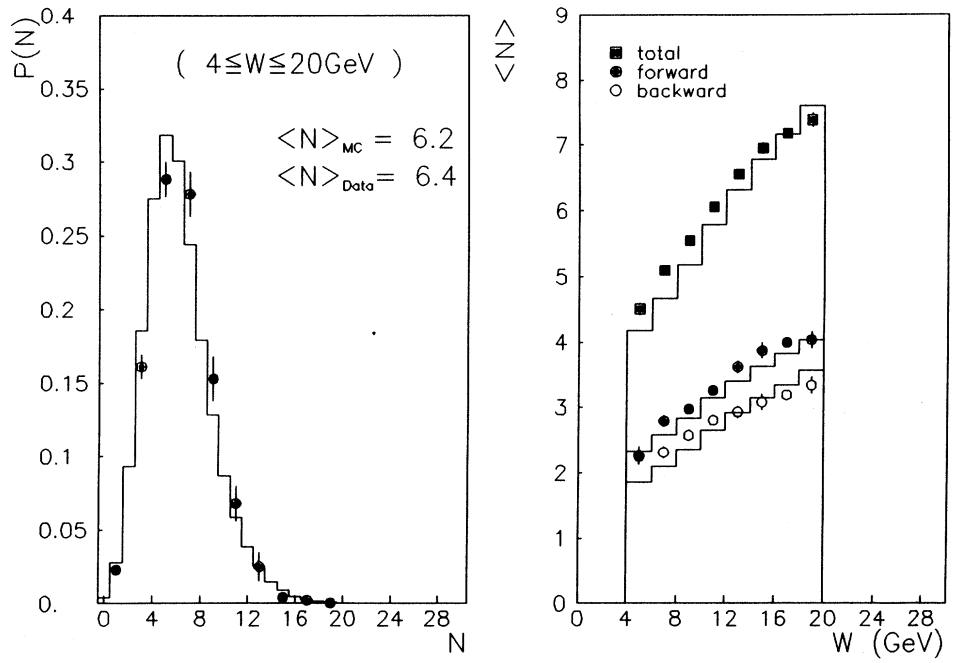

FIG. 7. (a) Multiplicity distribution of charged particles for all generated events ($4 < W < 20$ GeV) and (b) dependence of the mean multiplicity on the string energy W, separately for forward, backward, and total jet. Data from Ref. 13.

distribution function, does not allow us to describe the final baryon (proton) distribution with the same quality of agreement with data as we have obtained in e^+e^- fragmentation. Also the diquark string likes to emit mesons due to the larger phase space available for this process. Thus most baryons would be produced in the last emission step (by enforcing baryon-number conservation) and consequently would have low momentum in the string rest system. We did not find a way to overcome this problem without introducing further phenomenological

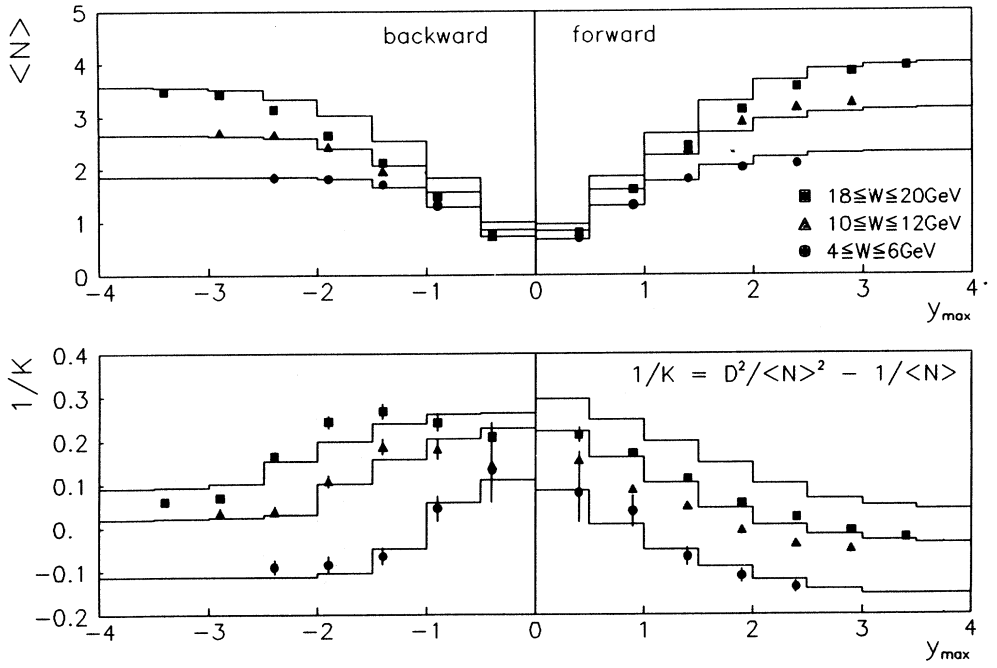

FIG. 8. The parameters $\langle N \rangle$ and $1/k$ of the multiplicity distributions in different rapidity windows $[0, y_{max}], [y_{min}, 0]$. The experimental values are obtained by fitting negative-binomial distributions to the experimental distributions. Data from Ref. 14.

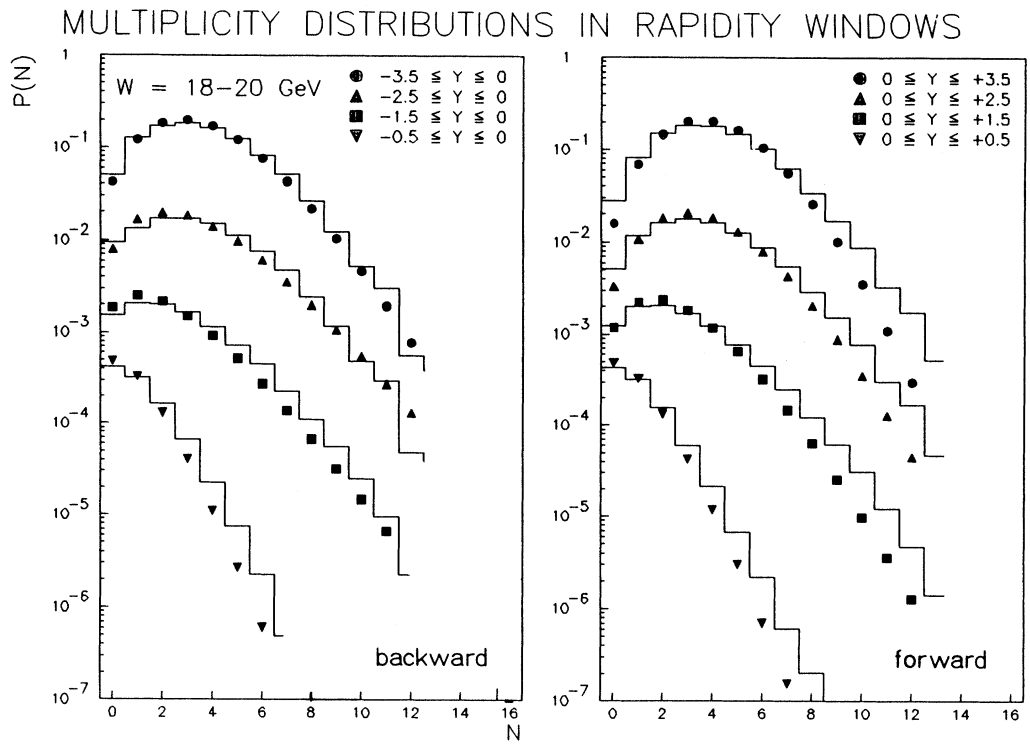

FIG. 9. The multiplicity distributions in different rapidity windows $[0,y_{max}],[y_{min},0]$. Consecutive plots are multiplied by factors of 0.1. The experimental values are obtained by fitting negative-binominal distributions to the experimental distributions in forward and backward direction. Data from Ref. 14.

parameters. As already mentioned this would require the possibility to investigate which values of Q^2 and W^2 cause the disagreement. The inclusive data are dominated by small W^2 values, i.e., small string energies, where the applicability of the string models may be questionable. Therefore we renounce the description of the baryon spectrum and treat the diquark fragmentation in a very simple way. In the first fragmentation step a proton or Λ (with equal probability) is emitted backwards with a constant rapidity distribution

$$\frac{dn}{dy}=[1/y_{max}(W)]\Theta(-y_{max}<y<0)$$

and

$$\frac{dn}{dp_T^2}\sim\exp[-p_T^2/0.2(\mathrm{GeV}/c)^2]\ .$$

This method cannot reproduce the measured proton spectra and related observables, but leads to a fairly good description of all other data. It also shows in which way the treatment of the proton fragmentation influences the other observables.

A. Results

We start with the display of a scatter plot of the generated events in the (Q^2,W^2) plane (Fig. 6). Projecting these events on the Q axis we see a strong peak at $Q^2\approx 15$ GeV^2. The projection on the W axis is rather flat for 100 GeV$^2<W^2<400$ GeV^2. All following theoretical distributions are obtained from these events by applying the same kinematical cuts as done experimentally.

Figure 7 shows the multiplicity distribution of charged particles for the whole kinematic range 4 GeV $<W<20$ GeV as well as the variation of the mean multiplicity with string energy. The energy dependence of both mean values and the multiplicity distribution are well described. This is also true for the multiplicity distributions in restricted rapidity intervals as can be seen from Fig. 8, where we display the mean value $\langle N\rangle$ and the "width" $1/k\equiv\sigma^2/\langle N\rangle^2-1/\langle N\rangle$ of those distributions for different string energies W. We compare with experimental values which are obtained by fitting negative-binominal distributions

$$P_N=\binom{-k}{N}(-p)^N(1+p)^{-k-N}$$

$$=\binom{N+k-1}{N}\frac{(\langle N\rangle/k)^N}{(1+\langle N\rangle/k)^{N+k}}\quad\text{with } p=\langle N\rangle/k \tag{39}$$

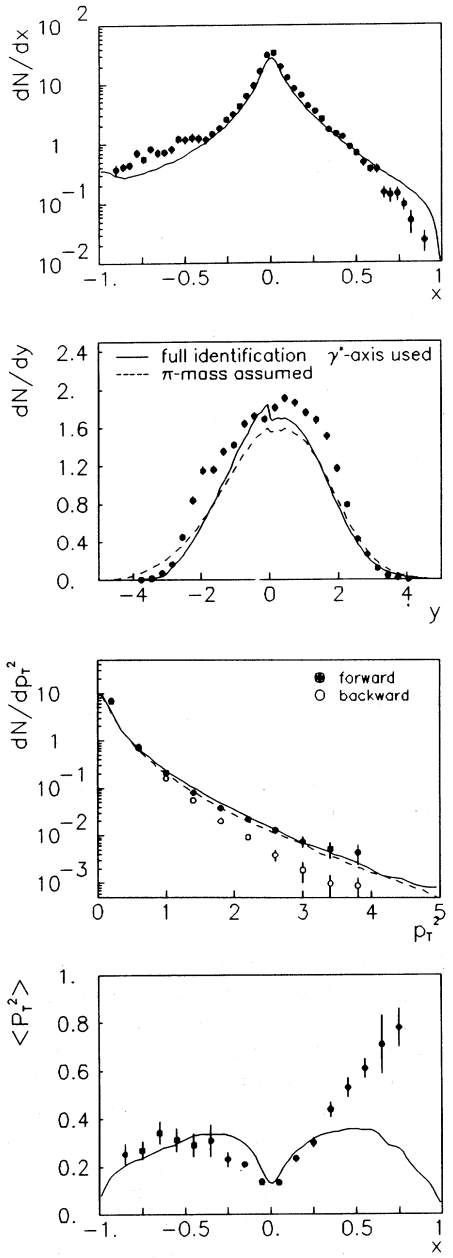

FIG. 10. Inclusive momentum distributions (relative to the virtual-photon axis) of charged particles from all generated events ($4 < W < 20$ GeV): (a) Feynman $x_L = 2p_L/W$ distributions; (b) rapidity distribution; (c) distribution of squared transverse momentum, separately for forward (solid line) and backward (dashed line) jet; (d) seagull plots $\langle p_T^2 \rangle(x_L)$. Data from Ref. 15.

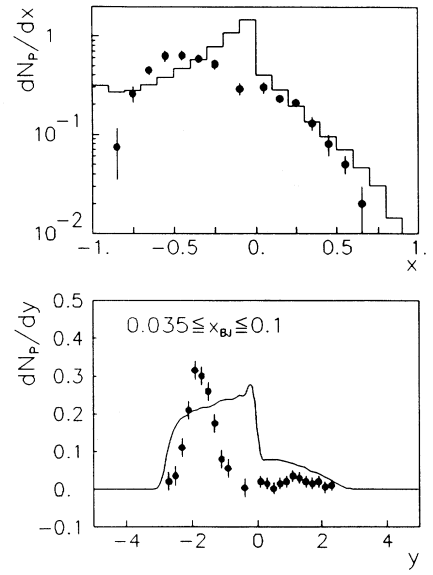

FIG. 11. Inclusive proton spectra: (a) $x_L = 2p_L/W$ distribution; (b) rapidity distribution; here only events with $0.035 < x_B < 0.1$ are selected and the data show the difference between protons and antiprotons. Data from Ref. 16.

to the data. The comparison with the whole distribution is displayed in Fig. 9. For the distribution in the limited rapidity interval the uncertainties due to incomplete particle identification are of the same order as the discrepancies between the data and the calculation. In all cases the mean values are well reproduced. In forward direction we overpredict the k value for large W. This parameter, however, is extremely sensitive to small changes of the distribution, especially to slight changes of the mean value, and may be also influenced by the experimental selection of the distribution.

We come now to the momentum distributions. In Fig. 10 we display the longitudinal- and the transverse-momentum distribution of charged particles. The $x = 2p_L/W$ distribution is quite nicely reproduced in forward and backward directions. It is therefore astonishing that we miss the integral of the rapidity distribution. This is due to the fact that the integral of the experimental distribution is not compatible with the mean multiplicity: $\int (dN/dy)dy \neq \langle N \rangle$. Since experimentally only part of the particles are identified (which cannot be modeled theoretically) we display two extremes: the distribution under the assumption that we have complete identification and under the assumption that all particles are pions. The transverse-momentum distribution is well reproduced in forward direction but gives values too large in backward direction. The seagull plot $\langle p_T^2 \rangle(x)$ is nearly symmetric and does not show the asymmetric rise in the forward jet. Sometimes this asymmetry is associated with stronger gluon radiation in the forward jet, which is not taken into account in our simple method of string formation.

As noted already, the important dynamical feature of the reaction is the fate of the proton remnant, i.e., the fragmentation of the diquark. A suitable observable to study this is the distribution of protons, shown in Fig. 11. Experimentally a characteristic maximum at $x_L \approx -0.5$,

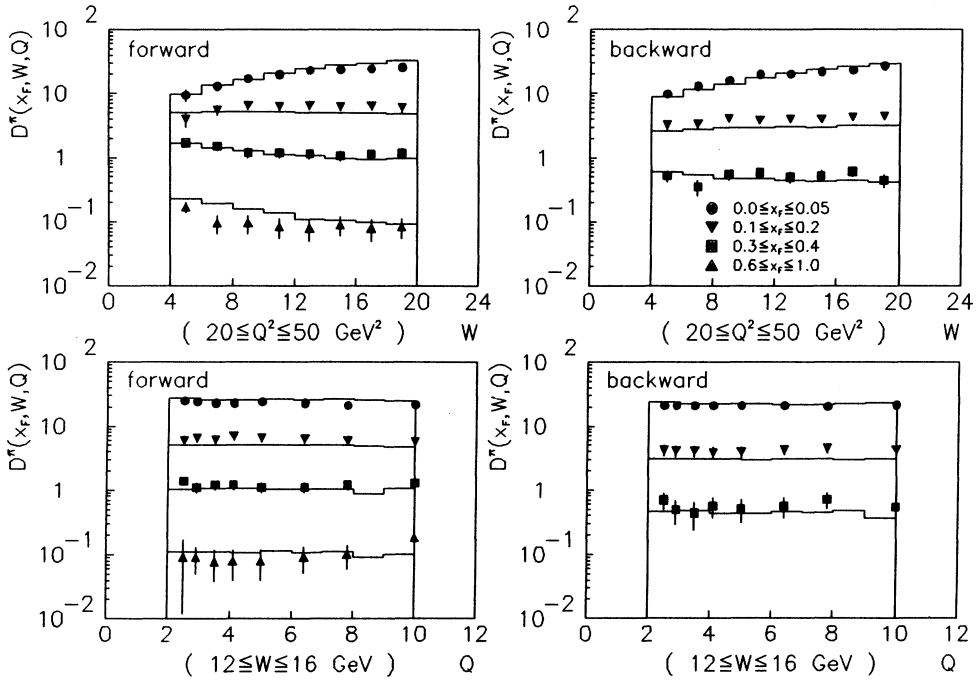

FIG. 12. Dependence of the pion fragmentation functions on the kinematical variables Q and W. Data from Ref. 17.

and $y \approx -2$ is seen. Our simple method of proton fragmentation would yield a nearly constant rapidity distribution in the backward jet at fixed string energy, but due to the contribution of string energies $4 < W < 20$ GeV a decreasing distribution results. In forward direction, where the creation of protons is given by the relative phase space, we are in good agreement with the data.

In spite of the insufficient treatment of the diquark fragmentation, the characteristics of pion production are very well described, as noted already for the multiplicity distributions. In Fig. 12 we show the Q and W dependence of the pion fragmentation functions. In our model string formation and fragmentation are treated independently and therefore the fragmentation functions are Q independent [apart from the negligible influence of the Q-dependent intrinsic parton transverse momenta, Eq. (38)]. The W dependence is more complex. For large momenta (large x_L) the distribution is independent of W; i.e., we observe scaling. At low momenta we observe the breakdown of the scaling. Our calculation is in almost perfect agreement with data. For the low values of x_L the scaling violation is already well described in the simplified analytical calculation [Eq. (13)]. For large x_l the formation of resonances becomes important as explained in Sec. III.

VI. APPLICATION TO PROTON-PROTON COLLISIONS

Motivated by the nice agreement with deep-inelastic lepton scattering data we proceed now to pp collisions. It has already been shown in Ref. 4 that soft proton-proton collisions and deep-inelastic lepton scattering can be described by the same model, based on the dual-parton model. We concentrate here on CERN ISR energies 31 and 62 GeV. For the formation of strings we follow the dual-parton model. In the simplest version of this model in a proton-proton collision a color exchange between two valence quarks of the protons takes place, leading to the formation of two (quark-diquark) strings identical to those in μp scattering (Fig. 13). At higher energies $\sqrt{s}$ color exchanges between sea quarks and gluons have to be taken into account. Because of the form of their structure function the created strings have a lower invariant mass. At ISR energies they can be neglected as well as hard parton-parton scattering processes.

For a quantitative calculation of the string formation

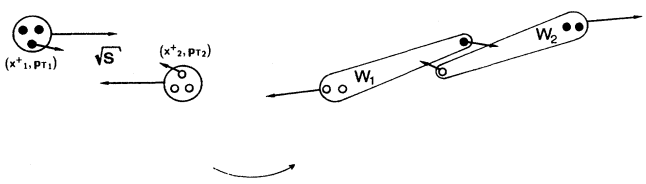

FIG. 13. An inelastic, nondiffractive proton-proton collision in the dual-parton model: By a color exchange between valence quarks two quark-diquark strings are formed.

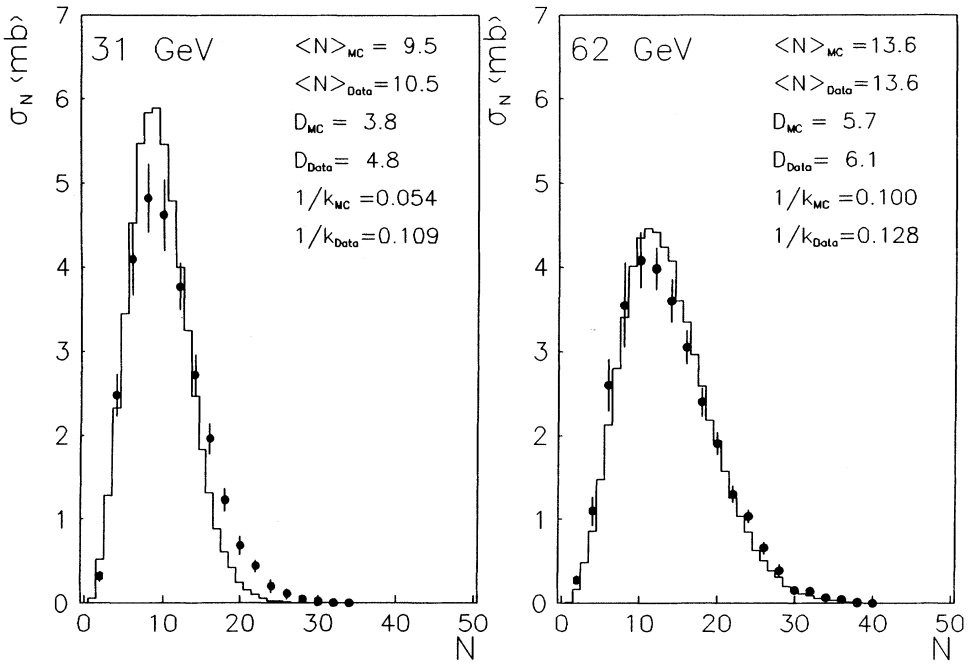

FIG. 14. Multiplicity distributions of charged particles for nondiffractive events in inelastic pp collisions at $\sqrt{s}=31$ and 62 GeV. Data from Ref. 19.

process the momentum distribution $f(x^+,\mathbf{p}_T)$ of the valence quarks in the proton is needed. We use the parametrization of Duke and Owens at the lowest possible $Q^2=4$ (GeV/c)^2 for the longitudinal parton density,

$$f_V(x^+)=1.88(x^+)^{-0.58}(1-x^+)^{3.46}(1+4.4x^+)\ , \qquad (40)$$

and generate transverse momenta by the method explained in Sec. IV.

This well-defined procedure avoids the problem of a cutoff: Taking the light cone x^+ as longitudinal momentum fraction of the parton we would have, for a given $\langle p_T^2\rangle$, the rather unphysical situation that infinitely many partons have almost zero longitudinal momentum but a finite transverse momentum. Taking the light cone x^+ as an energy fraction we are left with the problem of how to divide the total momentum into transverse and longitudinal momentum. Both assumptions yield quite different results.

Having determined the longitudinal and transverse momenta of the partons we can calculate the mass of a string with "end points" $(m_1,x_1,\mathbf{p}_{T_1})$ and $(m_2,x_2,\mathbf{p}_{T_2})$ as

$$\begin{aligned} W^2(m_1,m_2,x^+_1,x^+_2,\mathbf{p}_{T_1},\mathbf{p}_{T_2}) &= (p_1+p_2)^2 \\ &= x^+_1x^+_2P^{+2}+\frac{m^2_{T_1}m^2_{T_2}}{x^+_1x^+_2P^{+2}} \\ &\quad -2\mathbf{p}_{T_1}\cdot\mathbf{p}_{T_2}+m_1^2+m_2^2\ , \end{aligned} \qquad (41)$$

where P^+ is the proton light-cone momentum. We use quark and diquark masses of 0, M_{proton}, but the final results are insensitive to this choice. The string formation process is now completely specified and the fragmentation of the two generated strings is treated independently as described in Sec. V.

A. Results

We generated events at $\sqrt{s}=31$ GeV and $\sqrt{s}=62$ GeV to compare with ISR data for multiplicity and rapidity distributions of charged particles. Figure 14 shows multiplicity distributions for both energies. At 31 GeV the theoretical mean multiplicity is about one particle too low; at 62 GeV the agreement between theory and data is perfect. For higher collision energies the distribution widens up too strongly and cannot be described by 2-string formation alone.

Figure 15 shows rapidity distributions, for all events and also for selected "windows" of low and high multiplicity. The experimental data should taken with some care, since the acceptance of the detector reaches only up to $|\eta|<4$, as can be seen. Unfortunately we are not aware of more detailed investigations of the pp system at this energy.

VII. CONCLUSIONS

We developed a model for string fragmentation, based on the assumption that the color string decays sequential-

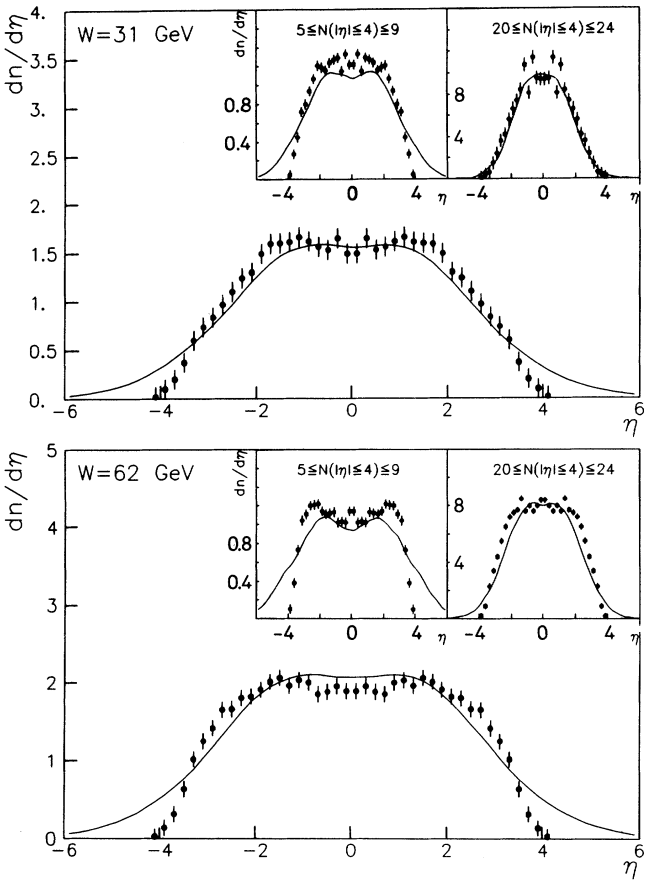

FIG. 15. Inclusive pseudorapidity distributions of charged particles in inelastic pp collisions at $\sqrt{s}=31$ and 62 GeV. Shown as insets are the rapidity distributions for events with multiplicities $5 \leq N \leq 9, 20 \leq N \leq 24$. Because of the detector acceptance only particles with $-4 \lesssim \eta \lesssim 4$ are seen. Data from Ref. 18.

ly and in each decay step a hadron is produced. Its momentum distribution is completely determined by the longitudinal phase space and one further parameter, the average transverse momentum of the produced hadrons. Because of the lack of knowledge of the meson resonances in the mass regions of the baryons one additional parameter, the meson-to-baryon ratio, is introduced by limiting the number of mesonic and baryonic species which we allow to be produced.

With this input we can describe a wealth of data measured in e^+e^-, μp, and pp collisions. This includes multiplicity distributions (total, in restricted rapidity and/or energy bins), the momentum distributions of different hadrons, the scale breaking of the pion momentum distribution at low Feynman x, and the production of higher resonances such as the η or the ρ meson.

From a physical point of view the result is rather disappointing. If phase space dominates the result, one can hardly learn anything about the transition matrix elements [Eq. (2)]. The agreement between our calculation and the data means that most inclusive single-particle data are insensitive to details of the fragmentation process, but rather sometimes biased by the experimental data analysis (as shown for the seagull plots in e^+e^- annihilation). Exceptions were the influence of three-jet events at higher energies in e^+e^- annihilation and the proton fragmentation in deep-inelastic scattering. Therefore it is certainly premature to conclude from an agreement between experimental data and models which employ QCD-inspired inputs such as counting rules that clear-cut information about the QCD is revealed.

The next step is an extension of this approach to proton-nucleus and nucleus-nucleus collisions. This requires additional parameters to describe the formation of strings in second and further collisions. Independently of that, a detailed investigation of two-particle correlation data is planned, in order to see whether two-body correlations such as the Hanbury-Brown–Twiss effect or strangeness compensation as a function of rapidity difference are equally well predicted in different fragmentation models or whether discrepancies with correlation data discard one or more of these approaches.

ACKNOWLEDGMENTS

This work has been funded in part by the German Federal Minister for Research and Technology (BMFT) under Contract No. 06 HD 710 and by the Gesellschaft für Schwerionenforschung (GSI).

[1]L. Van Hove, Nucl. Phys. **B9**, 331 (1969); W. Kittel, L. Van Hove, and W. Wojcik, Comput. Phys. Commun. **1**, 425 (1970); A. Krzywicki, Nuovo Cimento **32**, 1067 (1964); F. Lurçat and P. Mazur, *ibid.* **31**, 140 (1964); R. Baier *et al.*, *ibid.* **28A**, 455 (1975).

[2]Y. Kurihara, J. Hüfner, and J. Aichelin, Z. Phys. C **42**, 485 (1989).

[3]R. D. Field and R. P. Feynman, Nucl. Phys. **B136**, 1 (1978); B. Andersson, G. Gustafson, and B. Söderberg, Z. Phys. C **20**, 317 (1983); B. Andersson *et al.*, Phys. Rep. **97**, 31 (1983); CERN, Pool programs W5035/W5045/W5046/W5047/W5048 long writeup, 1987; L. Angelini *et al.*, Riv. Nuovo Cimento **6** (3), 1 (1983); E. Ferrari *et al.*, Z. Phys. C **41**, 39 (1988).

[4]A. Capella, U. Sukhatme, and J. Tran Thanh Van, Z. Phys. C **3**, 329 (1980); A. Capella and J. Tran Thanh Van, *ibid.* **10**, 249 (1981); **18**, 85 (1982); K. Werner, Phys. Lett. B **197**, 225 (1987).

[5]B. Andersson *et al.*, Nucl. Phys. **B281**, 289 (1987); A. Capella *et al.*, Z. Phys. C **33**, 541 (1987); J. Ranft and S. Ritter, *ibid.* **27**, 413 (1985); K. Werner, Phys. Lett. B **219**, 111 (1989).

[6]H. J. Schulze and J. Aichelin, Phys. Rev. D **39**, 3271 (1989).

[7]V. Weisskopf, Phys. Rev. **52**, 295 (1937).
[8]J. Schwinger, Phys. Rev. **128**, 2425 (1962); A. Casher, J. Kogut, and L. Susskind, Phys. Rev. D **10**, 732 (1974); T. Fujita and J. Hüfner, *ibid.* **40**, 604 (1989).
[9]J. Kogut and L. Susskind, Phys. Rev. D **9**, 697 (1974); **9**, 3391 (1974).
[10]D. W. Duke and J. F. Owens, Phys. Rev. D **30**, 49 (1984).
[11]M. Glück and E. Reya, Nucl. Phys. **145**, 24 (1978).
[12]T. Sloan, G. Smadja, and R. Voss, Phys. Rep. **162**, 45 (1988); EMC, J. J. Aubert *et al.*, Nucl. Phys. **B259**, 189 (1985).
[13]EMC, M. Arneodo *et al.*, Nucl. Phys. **B258**, 249 (1985); H. Schiemann, DESY Report No. F14-87-05, 1987 (unpublished).
[14]EMC, M. Arneodo *et al.*, Z. Phys. C **35**, 335 (1987).
[15]EMC, M. Arneodo *et al.*, Z. Phys. C **36**, 527 (1987); **35**, 417 (1987).
[16]EMC, M. Arneodo *et al.*, Z. Phys. C **35**, 433 (1987).
[17]EMC, M. Arneodo *et al.*, Z. Phys. C **31**, 1 (1986).
[18]W. Thomé *et al.*, Nucl. Phys. **B129**, 365 (1977).
[19]A. Breakstone *et al.*, Phys. Rev. D **30**, 528 (1984).